http://ansinet.com/itj

ITJ

ISSN 1812-5638

INFORMATION TECHNOLOGY JOURNAL

ANSInet
Asian Network for Scientific Information
308 Lasani Town, Sargodha Road, Faisalabad - Pakistan

Information Technology Journal 12 (24): 8058-8065, 2013
ISSN 1812-5638 / DOI: 10.3923/itj.2013.8058.8065

Blind Video Super-Resolution Reconstruction with Gaussian Blur Estimation

Fengqing Qin
Institute of Computer Science and Technology in Yibin University, Yibin, 644000, China

Abstract: In order to improve the spatial resolution of videos, utilizing the sub-pixel movement information between the low-resolution frames and the blur function of the imaging system, a blind video super-resolution reconstruction method is proposed. Firstly, through Taylor series expansion and least square solving method, the movement parameters between the adjacent frames in the sliding window are estimated from coarseness to fine. Secondly, according to the error-parameter curves generated through Wiener filter image restoration method, the parameters of the Point Spread Function (PSF) of the reference frame in the sliding window are estimated. Finally, super-resolution frames are reconstructed through Iterative Back Projection (IBP) algorithm. Experiments are performed on simulated low resolution images and standard test video and practical video, respectively. The results demonstrate the effectiveness of our approach and show the great importance of Gaussian blur estimation in video super-resolution reconstruction.

Key words: Blind video super-resolution, sub-pixel registration, point spread function, iterative back projection, wiener filter

INTRODUCTION

To acquire high quality video, cameras must work at a reasonable frame-rate and with a reasonable depth of field. These requirements impose fundamental physical limits on the spatial resolution of the gained video by current cameras. In order to improve the spatial resolution of videos, the direct way is to enhance the precision and stability of the imaging system. However, increasing the number of pixels of the detector will reduce the amount of the light and hence increase the noise and widening the aperture to increase the amount of light incident on the detector will significantly reduce the depth of field.

Super-resolution is an efficient approach to transcend the limitations of the optical imaging systems through digital image processing algorithms which is relatively inexpensive to implement (Tian and Ma, 2011). Video super-resolution refers to producing a high-resolution video from one or multiple low-resolution videos which has become one of the hot research areas in image processing and computer vision. Qin *et al.* (2009) proposed a segmental video super resolution reconstruction model and a framework of video super resolution reconstruction method based on sub-pixel registration and iterative back projection. (Qin *et al.*, 2009). Xiong *et al.* (2010) proposed a robust single-image super resolution method for enlarging low quality web image or video degraded by downsampling and compression (Xiong *et al.*, 2010). Keller *et al.* (2011) proposed an energy-based algorithm for motion-compensated video super-resolution targeted on upscaling of standard definition video to high-definition video (Keller *et al.*, 2011). Cheng *et al.* (2011) proposed a video super resolution reconstruction approach using a mobile search strategy and adaptive patch size (Cheng *et al.*, 2011). Zhang *et al.* (2012) proposed a SR framework for video sequence by extending the 2-dementional normalized convolution to 3-dimentional case (Zhang *et al.*, 2012). Chen *et al.* proposed a video SR using generalized Gaussian Markov random fields (Jin *et al.*, 2012).

In many practical applications, the restoration problem is always blind. This means that the blur function of the imaging system is most likely unknown or is known only some parameters of the Point Spread Function (PSF). In many super-resolution reconstruction algorithms, the more accurate the imaging system is estimated, the better performance the reconstruction algorithms will achieve. In most of the current algorithms, the motion and down sampling process of the imaging system are mainly considered and the sub-pixel movement information between the low-resolution frames is estimated to reconstruct a high-resolution frame. However, the blurring process of the imaging system is assumed to be a known PSF with given parameters in most algorithms, or is not considered at all in some algorithms. Both cases do not meet the real imaging model of the optical devices in practice. Blind video super-resolution reconstruction problem arises naturally and is expressed as estimating a high-resolution video and the blur function simultaneously. The foremost difficulty of blind de-blurring is rooted in the fact that the observed image

is an incomplete convolution. The convolution relationship around the boundary is destroyed by the cut-off frequency (Zou, 2004) which makes it much more difficult to estimate the blur function. Thus, blind super-resolution reconstruction has become one of the advanced issues and challenges in this technique and a satisfying solution to this problem has not been well solved yet (Giannoula, 2011; He *et al*., 2009).

The super-resolution reconstruction algorithms mainly include the frequency domain method and the spatial domain method. The latter is researched extensively and mainly includes non-uniform interpolation, adaptive filtering method, wavelet super-resolution etc. Among then, IBP has the virtues of small amount of calculation, fast convergent speed, automatically de-noising etc. It meets the real time requirement and can be well used in video super-resolution reconstruction. In IBP method, the estimated high-resolution frame is projected onto the low-resolution imaging model to generate multiple simulated low-resolution frames and then the simulation error is back-projected onto the high-resolution image grid. With the convergence of error, a super-resolution frame is gained. Thus, if the low-resolution imaging model is estimated more accurately, the quality of the reconstructed video will be better. In addition to estimate the movement between the frames accurately, the blur function of the imaging model needs to be estimated, but this is seldom done in many studys. As Gaussian PSF is the most common blur function in many imaging systems, the parameters of Gaussian PSF are estimated in this article. Utilizing Wiener filter image restoration algorithm,multiple error-parameter curves are generated at different parameters. By setting a threshold of the distance between curves, the size of the PSF is estimated and by setting a threshold of the increment on the estimated curve, the standard deviation of the PSF is determined. In Wiener filter algorithm, reflection symmetric extension is performed on the observed frame to restrain the parasitic ripple induced by the boundary cutof to enhance the performance of Wiener filter algorithm. This Gaussian blur estimation method may also be well utilized to handle other types of blur, only if the PSF can be denoted by parameters.

FRAMEWORK OF VIDEO SUPER RESOLUTION RECONSTRUCTION

In this study, Iterative Back Projection (IBP) super-resolution reconstruction method is adopted and the blur function of the imaging system is estimated to enhance the performance of IBP. The basic idea of IBP method is described as below. If the estimated high-resolution frame is closed to the original high-resolution frame, the simulated output low-resolution frames gained by the estimated high-resolution frame under the low-resolution imaging model will be consistent with the practical input low-resolution frames of the imaging system. Projecting the simulation error onto the high-resolution image grid, with the convergence of error, a super-resolution frame will be ultimately gained. Based on this idea, the schematic diagram of IBP is shown in Fig. 1.

where, $\hat{f}$ is the estimated high-resolution frame; P is the number of frames of the sliding window in video super-resolution reconstruction model; g_i, 1 = i = P, is the ith practically observed low-resolution frame; $\hat{g}_i$ is the ith simulated low-resolution frame of $\hat{f}$ under the low-resolution imaging model; $(\hat{g}_i - g_i)$ is the ith simulation error; E_i, C and D are the matrix forms of the motion, blurring and down sampling processes respectively; $^{-1}$ denotes the inverse operation; n_i is the ith

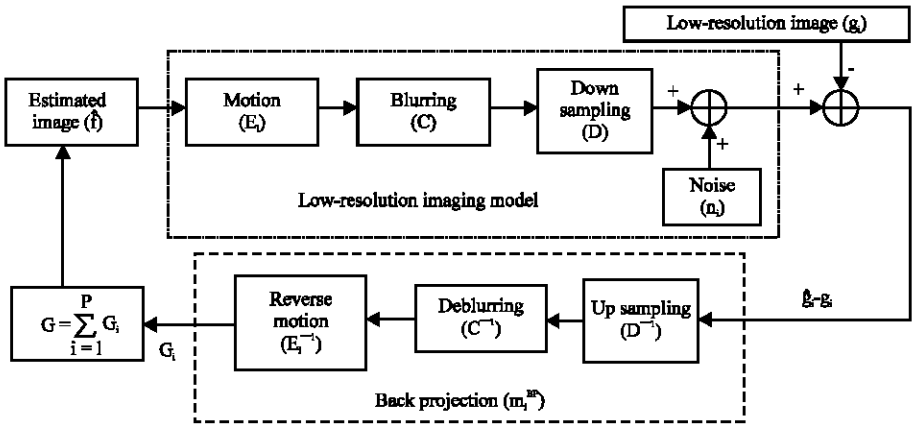

Fig. 1: The schematic diagram of iterative back-projection method

system noise; M_i^{BP} is the ith back projection operator; G is the summation of the back projections made by all of the simulated images on the high-resolution image grid in the current iteration.

According to Fig. 1, the low-resolution imaging model may be expressed in matrix forms as follows:

$$g_i = DCE_i\hat{f} + n_i = M_i\hat{f} + n_i,\ i \le i \le P \tag{1}$$

The mathematical description of IBP algorithm is expressed as:

$$\hat{f}^{k+1} = \hat{f}^k - \lambda\sum_{i=1}^{P} M_i^{BP}(\hat{g}_i - g_i) \tag{2}$$

where, k is the iteration number; $\hat{f}^k$ is the estimated high-resolution image in the kth iteration; λ is the gradient step. The relative error in the kth iteration is defined as:

$$\varepsilon^k = \left\|\hat{f}^{k+1} - \hat{f}^k\right\|^2 / \left\|\hat{f}_k\right\|^2 \tag{3}$$

The iteration process stops when the relative error is less than a given threshold or the maximum iteration number is reached.

In IBP algorithm, if the low-resolution imaging model is estimated much more accurately, the quality of the super-resolution video will be better. The simulation error relies on the imaging model greatly. The back projection operator is the key of the whole algorithm which ensures the convergence of the iterating process and makes the super-resolution reconstructed frame be closed to the original high-resolution frame. However, due to the ill-posed problem of the super-resolution reconstruction, it is very difficult to select this back projection operator. The best value of this operator is the reverse version of the low-resolution imaging model, namely, $M_i^{BP} = M_i^{-1}$. Thus, the back projection operation (M_i^{BP}) should include the processes of up-sampling (D^{-1}), de-blurring (C^{-1}) and reverse motion (E_i^{-1}). In most studys, the down-sampling and the motion processes of the imaging model are considered only. However, the blurring process of the imaging model is assumed to be a given PSF set by subjectively, or is even not considered at all. Both cases do not meet the real imaging model of optical devices. Thus, estimation error will increase and the quality of the reconstructed video will degrade. In the de-blurring process, the PSF of the imaging model needs to be estimated.

MOVEMENT REGISTRATION

The frame-to-frame movement registration algorithm is very important in the whole process and its precision is directly related to the quality of the reconstructed video. As only pure translational transformation exists between the adjacent frames in most videos, this case is considered in this article. Let the reference frame be r(u′, v′) and the image to be registered be s(u, v), the horizontal shift and the vertical shift between them are a and b respectively. The rigid transformation model between the coordinates of these two frames may be denoted as:

$$\begin{bmatrix} u' \\ v' \end{bmatrix} = \begin{bmatrix} u \\ v \end{bmatrix} + \begin{bmatrix} a \\ b \end{bmatrix} \tag{4}$$

Then, the mathematical relationship between these two frames can be expressed as:

$$s(u,v) = r(u',v') = r(u+a, v+b) \tag{5}$$

Two dimensional series expansion at (u,v) is made to the right part of Eq. 2. Ignoring the high order terms, the following approximate expression is gained:

$$s(u,v) \approx r(u,v) + a\frac{\partial r}{\partial u} + b\frac{\partial r}{\partial v} \tag{6}$$

It may be rewritten as:

$$AX = B,\ A = \begin{bmatrix} \frac{\partial r}{\partial u} & \frac{\partial r}{\partial v} \end{bmatrix},\ X = \begin{bmatrix} a \\ b \end{bmatrix},\ B = s(u,v) - r(u,v) \tag{7}$$

The solution of Eq. 4 can be solved through least square method and the optimal estimated movement parameters are $\hat{X} = [\hat{a}\quad \hat{b}]^t$, where, $\hat{a}$ is the estimated horizontal shift, $\hat{b}$ is the estimated vertical shift and t is the transpose operator.

On one hand, in order to improve the computing speed and enhance the robustness to noise, three-level Gaussian pyramid image models are formed to the reference frame and the frame to be registered respectively. The movement parameters are estimated from coarseness to fine. On the other hand, in order to improve the precision of the registration algorithm, the movement parameters are estimated through an iterative approach in each level. In this method, the coarse levels with low-resolution are used to determine the big movement information and the fine level with high-resolution is used to adjust the estimated movement

parameters accurately. In this way, the optimal movement parameters with high sub-pixel precision will be obtained.

GAUSSIAN BLUR ESTIMATION

Gaussian point spread function (PSF) is the most common blur function of many optical measurements and imaging systems. Thus, the estimation of Gaussian PSF is mainly considered in this article. Generally, the Gaussian PSF is expressed as:

$$h(m,n)=\begin{cases}\frac{1}{\sqrt{2\pi}\sigma}\exp\{-\frac{1}{2\sigma^2}(m^2+n^2)\} & (m,n)\in R\\ 0 & \text{others}\end{cases} \quad (8)$$

where, σ is the standard deviation; R is a supporting region. Commonly, R may be denoted as a K×K rectangular region, where, K is called as the size of the PSF and is often an odd number.

From Eq. 8, we can see that two parameters need to be estimated for the Gaussian PSF, namely, the size (K) and the standard deviation (σ). Because the Fourier transformation of a Gaussian function is still a Gaussian function, it is impossible to determine these parameters by the zero-crossing point in the frequency domain. But in many cases, the isolated point and the intensity edges in the observed image may provide the necessary information to estimate the PSF. If the image and the noise are assumed to be generalized stationary process, then the Discrete Fourier Transform (DFT) method and Wiener filter are used to estimate the restored image:

$$X=\frac{H^*Y}{|H|^2+S_{nn}/S_{xx}} \quad (9)$$

where, X, Y and H are the DFT of the real image x, the blurred image y and the blur function h respectively; * denotes the conjugate operation; S_{nn} and S_{xx} denote the power spectrum of the noise and the real image respectively. As it is usually very difficult to estimate S_{nn} and S_{xx}, X is usually approximated by the following formula:

$$X=\frac{H^*Y}{|H|^2+\Gamma} \quad (10)$$

where, Γ is a positive constant. The best value of Γ is the reciprocal of the SNR of the observed image.

In Wiener filter restoration algorithm, in order to restrain the parasitic ripple induced by the boundary cutoff, the image needs to possess circular boundary. For an observed image of size M×N, reflection symmetric extension is performed on it to produce an extended image of size 2M×2N and calculate its DFT Y. Given a size K of the PSF, the error-parameter curve is generated at different standard deviation σ. According to the error-parameter curves at different sizes, these two parameters can be estimated approximately. The estimation criteria is as below: the size where the distance between the curves decreases evidently is assumed to be the estimated size and the standard deviation where the corresponding curve increases obviously is assumed to be the estimated standard deviation. Thus, we can set two thresholds T_1 and T_2 to estimate these two parameters. Firstly, given an estimation error e, the curve where once the distance between curves is smaller than T_1 gives out the estimated size $\hat{K}$ of the PSF. The distance is defined as the absolute difference of the cycle number (j) of standard deviation at e. Then, the deviation value needs to be estimated which can be done by calculating the increment of the estimation error at different standard deviations on the estimated curve. The deviation once the increment is greater than the threshold T_2 is the estimated deviation $\hat{\sigma}$. When the original sizes of K are taken as 3, 5, 7, 9, 11 and 13, the Gaussian PSF estimation process is expressed as follows:

- **Step 1:** Select a standard deviation range given by the minimum value σ_{min} and the maximum value σ_{max} and Set a searching number S, then $\Delta\sigma = (\sigma_{max}-\sigma_{min})/S$
- **Step 2:** Set the original sizes: K(1) = 3, K (2) = 5, K (3) = 7, K(4) = 9, K(5) = 11, K(6) = 13
- **Step 3:** For i = 1:6, execute Step 4; Otherwise, jump to Step 5
- **Step 4:** For j = 1:S, execute Step 4.1to Step 4.5; Otherwise, jump to Step 3
  - **Step 4.1:** Compute the current standard deviation: $\sigma = \sigma_{min}+(j-1)/\Delta\sigma$
  - **Step 4.2:** According to Eq. 8, generate the PSF h of size K(i) and standard deviation σ
  - **Step 4.3:** Extend h to be the size of 2M×2N by adding zeros and compute its DFT H
  - **Step 4.4:** According to Equation (10), estimate the DFT of the real image X
  - **Step 4.5:** Compute the estimation error: $E(i, j) = \|Y-YH\|^2$ and normalize it
- **Step 5:** Plot the error-parameter (E-σ) curves at different sizes K
- **Step 6:** Give an estimation error e and calculate the distance between curves. The curve once the distance d is smaller than the threshold T_1 represents the real parameters, from which the size $\hat{K}$ of the PSF is estimated
- **Step 7:** Calculate the increment at different standard deviations on this curve. Once the increment is greater than the threshold T_2, the deviation $\hat{\sigma}$ of the PSF is estimated

EXPERIMENTS

Experiments on simulated low-resolution images: In order to test the performance of the algorithms in this article, experiment is firstly performed on multiple simulated low-resolution images.

For the test image 'lena' of size 256×256, in order to avoid the boundary effect caused by the motion process, a zero window of size 16 pixels is added around the original image. The gained image of size 288×288 is the simulated high-resolution image as shown in Fig. 2.

According to the low-resolution imaging model in Fig. 1, five simulated low-resolution images are generated. Firstly, this high resolution image is horizontally shifted by a_0 and vertically shifted by b_0 according toe the parameters in Table 1. Secondly, the shifted images are convolved with a Gaussian PSF to simulate the blur process. The original size K_0 of PSF is 7 and the original standard deviation σ_0 is 1.2. Thirdly, the gained images are down sampled by a factor of 2. Finally, Gaussian zero-mean white noise is added to each blurred images at 40 dB blurred signal-to-noise ratio (BSNR), where, the BSNR is defined as:

$$BSNR = 10\log_{10}(\text{Variance of the blurred image/Variance of noise}) \quad (11)$$

Taking the first image as the reference image, movement registration is carried out to estimate the horizontal shift $\hat{a}$ and the vertical shift $\hat{b}$. The absolute estimation errors are used to evaluate the precision of the registration algorithm. The horizontal and vertical absolute estimation errors are defined as:

$$\Delta a = |a_0 - \hat{a}|$$

And:

$$\Delta b = |b_0 - \hat{b}|$$

respectively. The gained estimation absolute errors are shown in Table 2. The result shows that this registration algorithm can achieve high sub-pixel precision.

The Gaussian PSF of the reference image is estimated through the proposed method in Section ¢õ. The original sizes of PSF are taken as 3, 5, 7, 9, 11 and 13. The searching number S is taken as 50. The range of the standard deviation is taken as [0.5,2], namely, $\sigma_{min} = 0.5$, $\sigma_{max} = 2$. The estimation error e is 0.1. The thresholds are $T_1 = 3$ and $T_2 = 0.015$. The error-parameter curves of the reference image are shown in Fig. 3 which can represent the parameters of the PSF approximately. The estimated size $\hat{K}$ of the PSF is 7 and the estimated standard deviation $\hat{\sigma}$ is 1.19. The size of the PSF is estimated

Fig. 2: The high-resolution image

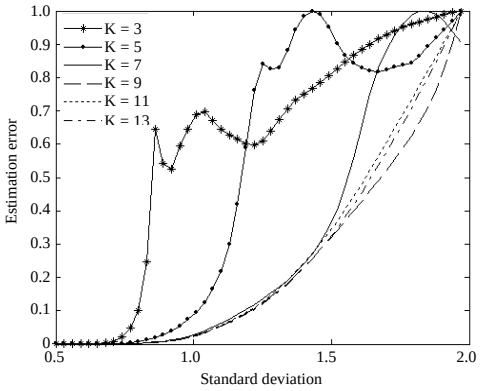

Fig. 3: The error-parameter curves of the reference image

Table 1: The original movement parameters

Sequence No. (i)	Horizontal shift (a_i) (in pixel)	Vertical shift (b_i) (in pixel)
1	0	0
2	-8.6974	-5.0926
3	4.0909	7.1342
4	-5.2904	6.5494
5	8.6912	-7.3714

Table 2: The estimated absolute estimation errors

Sequence No. (i)	Horizontal shift (a_i) (in pixel)	Vertical shift (b_i) (in pixel)
1	0	0
2	0.0047	0.0018
3	0.0014	0.0014
4	0.0027	0.0052
5	0.0038	0.0046

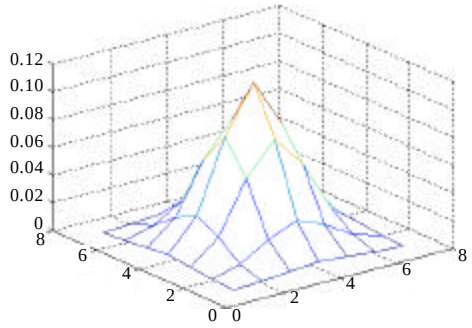

Fig. 4: The estimated PSF ($\hat{K}$ = 7, $\hat{\sigma}$ = 1.19)

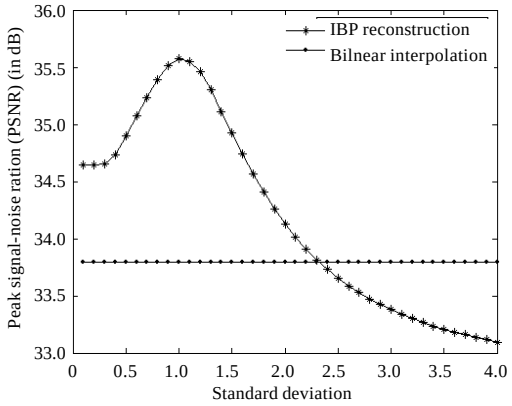

Fig. 5: The PSNR of the reconstructed at different standard deviations ($\hat{K}$ = 7)

correctly and the estimation relative error of the standard deviation ($|\hat{\sigma} - \sigma_0|/\sigma_0$)) is 0.0083. The estimated PSF is shown in Fig. 4.

Utilizing the sub-pixel movement information between the low-resolution images and the estimated PSF of the reference image, super-resolution image is reconstructed through IBP algorithm. In order to verify the influence of the PSF estimation on the quality of the reconstructed image, while the estimated size $\hat{K}$ of the PSF is 7, super-resolution reconstruction is carried out at different estimated standard deviation $\hat{\sigma}$ and the corresponding PSNR of the super-resolution reconstructed image is shown in Fig. 5. We can see that the PSNR is the highest around the real values of the PSF. If the parameters of the PSF are far away from the real values, the PSNR decreases greatly. When the estimated standard deviation is greater than 2.3, the PSNR of the super-resolution reconstructed image is even lower than that of the amplified image by Bilinear interpolation to the reference image only.

The amplified image by Bilinear interpolation to the reference image with a factor of 2 is shown in Fig. 6a.

Fig. 6(a-d): The reconstructed images through bilinear interpolation and super-resolution at different standard deviations ($\hat{K}$ = 7), (a) Bilinear interpolation (PSNR = 33.7897 dB), (b) SR image ($\hat{\sigma}$ = 0.1, PSNR = 34.6452 dB), (c) SR image ($\hat{\sigma}$ = 1.19, PSNR = 35.4701 dB) and (d) SR image ($\hat{\sigma}$ = 4, PSNR=33.0961 dB)

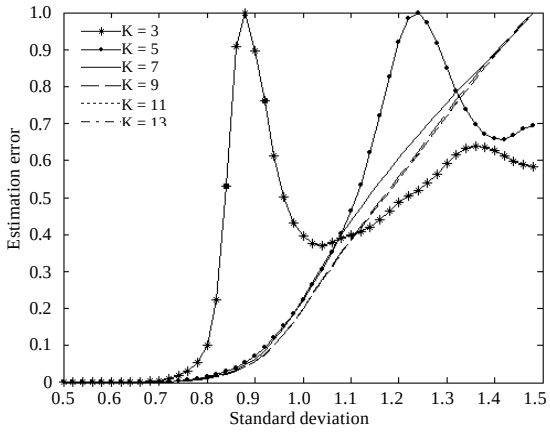

Fig. 7: The error-parameter curves of the reference frame

When the estimated size $\hat{K}$ of the PSF is 7 and the estimated standard deviation $\hat{\sigma}$ is taken as 0.1, 0.5, 1.19, 2 and 4, respectively, the corresponding super-resolution reconstructed images are shown in Fig. 6 (b)~(d). From the visual effect of the reconstructed image, we can see that when the parameters of the PSF are estimated much more accurately, the reconstructed image will be much more closed to the real high-resolution. Otherwise, the quality of the reconstructed image will degrade greatly. When $\hat{\sigma}$ is around the real value, the super-reconstructed reconstructed image (c) has the best visual effect. When $\hat{\sigma}$ is much lower than the real value, the reconstructed image (a) is blurred and illegible. When $\hat{\sigma}$ is much larger than the real value, ringing artifact and ghost effect are very obvious in the reconstructed image (d).

Blind video super-reconstruction reconstruction: According to the video super-resolution reconstruction model, the first 100 frames in the standard test video 'clair.avi' are reconstructed. The size of each low-resolution frame is 88×72×3 pixels. The up-sampling factor is 2. This means the size of each reconstructed frame is 176×144×3 pixels. The number of frames of the sliding window P is taken as 5. The iteration number of IBP is taken as 10. The original sizes of the PSF are taken as 3, 5, 7, 9, 11 and 13. $\sigma_{min} = 0.5$, $\sigma_{max} = 1.5$, S = 50, e = 0.1, $T_1 = 3$, $T_2 = 0.015$.

For convenient description, take the super-resolution reconstruction of the 20th frame in this video as an example. Utilizing the proposed PSF estimation algorithm, the error-parameter curves of the reference frame in the 20th sliding window are shown in Fig. 7 and the estimated parameters of the PSF are: $\hat{K} = 5$ and $\hat{\sigma} = 0.88$.

The 20th amplified frame by Bilinear interpolation is shown in Fig. 8a. When the estimated size $\hat{\sigma}$ of the PSF is 5, the reconstructed frame at different standard deviations $\hat{\sigma} = 0.1$, $\hat{\sigma} = 0.88$ and $\hat{\sigma} = 3$ are shown in Fig. 8b-d, respectively. The experimental result justifies the importance of the PSF estimation in the quality of the

Fig. 8(a-d): The 20th reconstructed frames through bilinear interpolation and super-resolution at different standard deviations ($\hat{\sigma} = 5$), (a) Bilinear interpolation, (b) Super-resolution ($\hat{\sigma} = 0.1$), (c) Super-resolution ($\hat{\sigma} = 0.88$) and (d) Super-resolution ($\hat{\sigma} = 3$)

super-resolution econstructed frame again. When the estimated parameters are around the real values, the reconstructed frame (c) has the best visual effect. If the estimated parameters are far away from the real value, the reconstructed frame is illegible (b), or the ringing artifact and ghost effect are obvious in the reconstructed frame (d).

CONCLUSTIONS

A framework of blind video super-resolution method is proposed. The low resolution imaging model mainly includes movement, Gaussian blur and noise. The video reconstruction model, the movement registration algorithm, the super-resolution reconstruction algorithm and the PSF estimation method are researched. Experiments are performed on simulated low-resolution images and standard test video respectively. The results demonstrate the reliability and effectiveness of the proposed method. This registration algorithm achieves high sub-pixel precision. The size and standard deviation of the Gaussian PSF are estimated accurately through the proposed PSF estimation method. It can also be extensively used to handle other types of blur (such as motion blur and defocus blur). Both the PSNR of the super-resolution reconstructed image and the visual effect of the super-resolution video show the great importance of the Gaussian blur estimation in super-resolution reconstruction.

ACKNOWLEDGMENTS

This study is supported in part by the National Nature Science Foundation of China (Gant No. 61202195), the Sichuan Provincial Education Department project (Gant No. 11ZA174), the Application Fundamental Research Project of Sichuan Provincial Scientific and Technology Department (Gant No.2011JY0139), the key project of Yibin Science and Technology Bureau (Gant No. 2011SF016, 2013ZSF009).

REFERENCES

Cheng, M.H., H.Y. Chen and J.J. Leou, 2011. Video Super-resolution reconstruction using a mobile search strategy and adaptive patch size. Signal Process., 91: 1284-1297.

Giannoula, A., 2011. Classification-based adaptive filtering for multiframe blind image restoration. IEEE Trans. Image Process., 20: 382-390.

He, Y., K.H. Yap, L. Chen and L.P. Chau, 2009. A soft MAP framework for blind super-resolution image reconstruction. Image Vision Comput., 27: 364-373.

Jin, C., J. Nunez-Yanez and A. Achim, 2012. Video Super-resolution using generalized gaussian markov random fields. IEEE Signal Process. Lett., 19: 63-66.

Keller, S.H., F. Lauze and M. Nielsen, 2011. Video Super-resolution using simultaneous motion and intensity calculations. IEEE Trans. Image Process., 20: 1870-1884.

Qin, F.Q., X.H. He, W.L. Chen, X.M. Yang and W. Wu, 2009. Video superresolution reconstruction based on subpixel registration and iterative back projection. J. Electron. Imaging, Vol. 18. 10.1117/1.3091936

Tian, J. and K.K. Ma, 2011. A survey on super-resolution imaging. Signal Image Video Process., 5: 329-342.

Xiong, Z., X. Sun and F. Wu, 2010. Robust web image/video super-resolution. IEEE Trans. Image Process., 19: 2017-2028.

Zhang, K., G. Mu, Y. Yuan, X. Gao and D. Tao, 2012. Video Super-resolution with 3D adaptive normalized convolution. Neurocomputing, 94: 140-151.

Zou, M.Y., 2004. Deconvolution and Signal Recovery. Defense Industry Publishing, China.